This article has been accepted for publication in a future issue of this journal, but has not been fully edited. Content may change prior to final publication. Citation information: DOI 10.1109/TNSRE.2016.2613412, IEEE Transactions on Neural Systems and Rehabilitation Engineering

A method for removal of deep brain stimulation artifact from local field potentials

Xing Qian, Yue Chen, Yuan Feng, Bozhi Ma, Hongwei Hao, and Luming Li

***Abstract*—This article presents a signal processing method for the electrophysiology simultaneously recorded during deep brain stimulation (DBS) as a research tool. Regarding the local field potential (LFP) signals recorded during stimulation, a novel method was proposed for removal of stimulation artifacts caused by the much stronger stimulating pulse compared to typical LFP. This artifact suppression method was tested and evaluated in an *in vitro* situation. The results indicate that the stimulation artifacts are well suppressed by this method. Secondly, this method was tested *in vivo* in Parkinson's disease (PD) patients. It was used to process the LFP signals recorded intraoperatively from PD patients to preliminarily explore the quantitative dependencies of beta band synchronization variations in the subthalamic nucleus (STNs) on the applied DBS parameters, including stimulation voltage, frequency and pulse width. The results confirm that DBS therapy can suppress excessive beta frequency activity and that the degree of attenuation increases with increasing DBS voltage within a range of 1 to 3 V and increasing DBS frequency within a range of 60 to 120 Hz. The proposed artifact suppression method provides technical support for exploring the direct effect of electrical stimulation on the brain activities.**

***Index Terms*—deep brain stimulation (DBS), local field potential (LFP), artifact removal, Parkinson's disease**

I. Introduction

Over the past few decades, DBS has offered dramatic therapeutic benefits when long-term pharmacotherapy does not provide relief of the advanced symptoms in the treatment of movement disorders such as Parkinson's disease (PD)[1]. However, the biological mechanism underlying DBS is not known [2]. In addition to providing critical symptomatic relief for patients, DBS affords a unique and rare opportunity for exploring the electrical oscillatory activities in deep brain structures by recording the local field potentials (LFPs) directly from the DBS electrodes implanted into the specific target [3, 4]. LFPs may contain key information about functional activities of brain structures that may be associated with disease symptoms [5-7]. Evidence shows that DBS does not only affect neural tissue at the site of the electrodes, but disrupts pathological signals that reverberate through multiple brain regions. Thanks to DBS, humans have entered the era of human neural network modulation [8].

It is highly important to record the immediate LFP response in DBS whether for studying the neural network modulation mechanism of this therapy, or in the exploration of the closed-loop DBS systems [15, 16, 17], which is in the contrary to open-loop DBS, the mode giving constant high frequency electrical stimulation commonly used in clinical practice. Also, as there is an increase in the aging populations and the number of brain disorders, the monitoring of brain electrophysiological activities and how the stimulation influences the brain activities when the patients are receiving the DBS therapy is important. However, the amplitude of the stimulation pulses is too large compared to the neural activities, making the concurrent sensing during the stimulation difficult. It is full of challenges to inhibit the strong stimulation pulses as well as reserving the full information of the neural activities. So far, only Medtronic Inc. [18] provided an implantable system with concurrent sensing and stimulation called Activa PC+S, providing a research tool to investigate neural circuits while providing DBS therapy. This was the first time for really getting an insight into human brain functional activity [19].

Our previous work[20] describes the design of an implantable EEG device based on many years' experience developing DBS devices that not only provide the DBS therapy but also gives good measurements as a fundamental research tool. However, there are some residual stimulation artifacts in the signal recorded during the stimulation ON. This is unavoidable due to the restriction of the implantable device, including the space and power consumption. Therefore, a technique is needed to suppress the residual DBS artifacts during the following off-line data processing.

The DBS artifacts usually induce very highly strong spectral peaks at the stimulation frequency and its harmonics. Several methods have been used to suppress DBS artifacts in physiological signals recorded during concurrent DBS in previous studies. Low-pass or notch filters are straightforward solution. However, if the stimulation peaks overlap many frequency bins, these filters are not appropriate[21]. Other studies addressing DBS artifact suppression have concentrated on the template subtraction techniques [22]. However, the template subtraction techniques suffer from the assumptions

This work was supported by National Natural Science Foundation of China (No. 61601258, 81527901 and 51407103), Beijing Municipal Science & Technology Commission (No. Z151100003915123), The National Key Research and Development Program of China (No. 2016YFC0105502 and 2016YFC0105900), Major Achievements Transformation Project Of Beijing's College and Tsinghua University Initiative Scientific Research Program.

Xing Qian is with the National Engineering laboratory for Neuromodulation, Tsinghua University; Man-machine-environment engineering Institute, School of Aerospace Engineering, Tsinghua university (e-mail: qx10@ mails.tsinghua.edu.cn).

Corresponding author Luming Li is with the National Engineering laboratory for Neuromodulation, Tsinghua University; Man-machine-environment engineering Institute, School of Aerospace Engineering, Tsinghua university; Precision Medicine & Healthcare Research Center, Tsinghua-Berkeley Shenzhen Institute; Center of Epilepsy, Beijing Institute for Brain Disorders (e-mail: lilm@ mail.tsinghua.edu.cn).

that the artifact shape is constant between stimulation pulses. Thus, the template subtraction techniques are commonly used in extracellular recordings with high sampling rates to avoid the loss of high-frequency components. For instance, Hashimoto et al. [22] constructed a stimulus artifact template by averaging across all the peri-stimulus segments. However, the sampling rate of the ADC modules in implantable systems usually would not exceed 1 kHz because of the low power requirements of implantable medical devices. For instance, the Activa PC+S system used a sampling frequency of just 422 Hz [18]. With such a low sampling rate, each stimulus artifact will contain only several sampling points and have a different morphology and the template subtraction technique will be difficult to implement.

In the present work, we sought to develop a novel method to remove the DBS artifact based on stimulus artifact template reconstruction and subtraction, to keep the physiological signal in LFPs recorded during concurrent DBS. The method was assessed through *in vitro* experiments, in which mock LFPs were recorded with and without the stimulation to characterize the artifact suppression. The method was then used to process the LFPs that were recorded *in vivo* from the STN of PD patients during DBS surgery, with the signal characteristics dependent on the stimulation parameters.

II. Methods

A. Instrumentation Design and Implementation

The short distance between the four electrodes and the large amplitude of the electrical pulses, usually five to six orders of magnitude larger than that of the field potentials around the electrode, made it difficult to simultaneously record the LFPs during the DBS. Previous studies have used the symmetric geometry to record differential LFPs across nearest neighbor electrodes on the same lead with unipolar stimulation [9, 18]. With this electrodes configuration method, the distance from the stimulator case to the DBS lead is much greater than the space between the electrodes, so the two recording electrodes sense approximately the same stimulation pulses. The stimulation interference can then be seen as a common mode disturbance to the input amplifier. This study also used this symmetric geometry as shown in Figure 1. The monopolar stimulation mode was used with a titanium stimulator case as the positive electrode and one of the two middle contacts as the negative electrode. The negative electrode also served as the ground electrode for the LFP sensing module. A previous study has used bipolar stimulation [28] when recording DBS evoked LFP, applying stimulation pulses between electrode 4+ and 2- while recording differential LFP between electrode 1 and 3. Although this unsymmetrical configuration theoretically will bring larger artifacts into the recorded data, it is feasible as long as the ADC is not saturated and the real signal could be restored in the following processing. A passive filter network with a pass band of 0.3 Hz to 100 Hz suppressed the high amplitude (up to 10 V) stimulus signal to just several hundred microvolts, within the common-mode input range of the ADS1299 [23]. The ADS1299 produced by Texas Instruments is a programmable, low-noise, 24-bit analog front-end for biopotential measurements which contains eight channels of delta-sigma ADCs. The primary internal cells of the delta-sigma converters in the ADS1299 are the delta-sigma modulator with a very high modulation frequency at 1.024 MHz and a digital/decimation filter which is a third-order low-pass sinc filter with a variable decimation rate. The on-chip decimation filters also provide anti-aliasing filtering as well as filtering out high frequency noise.

The LFP sensing module is designed to be integrated into the implantable rechargeable neurostimulator with bilateral pulse output. The recorded data will be read out using RF communication in real time. The wireless recharging could be a trade-off for the additional power consumption of the LFP recording and transmission functions. The system can acquire up to four to five hours two-channel signal at a sampling rate of 1000 Hz on a single battery charge.

B. In vitro experimental setup

The system was tested in an *in vitro* setup to reproduce the stimulation/recording conditions of the DBS electrode within the brain, as shown in Figure 1. The DBS lead was a model L301 (Pins Medical, CHA) with four platinum–iridium cylindrical contacts (1.3 mm diameter and 1.5 mm length, spaced 0.5 mm apart, and span a total distance of 7.5 mm), numbered 1 to 4 from the most caudal to the most rostral contact. A Pins L301 DBS lead was immersed into a glass container filled with saline solution (9 g of NaCl per liter of water) at room temperature and was used to deliver monopolar stimulation and to record signals between the adjacent non-stimulating contacts. Two additional Ag/AgCl disc-electrodes which were usually used for recording scalp EEG were used to inject sinusoidal simulated LFP generated by a waveform generator (Tektronix, AFG310) into the saline solution. Given that the frequency spectrum of the beta power of the LFPs of PD patients is in the 14 Hz to 30 Hz band, a 23Hz sinusoidal was used to simulate the LFP signal. A custom program written in C# (Visual Studio) operated the components in the data acquisition module to setup the digital output timing and the signal sampling (by default, 1 kHz sampling rate). Contact 2 was used as the stimulation cathode with the stimulator case as the anode, and the differential signal was recorded between contact 1 and 3 to study the LFPs of the STN with a symmetrical distribution around the stimulating contact. According to neurosurgeons, monopolar stimulation is commonly used for therapy and contacts 2 and 3 are commonly placed within the STN. Hence, this electrode configuration is reasonable for the following *in vivo* intraoperative recording after completion of lead implantation. However, although DBS surgergical procedures attempt to place contacts 2 and 3 within the STN according to surgeons, the leads may move after surgery, inducing variability in the contacts. Therefore, patients applicable for the implantable recording will be restricted. Another limitation of the differential recording on the two contacts adjacent to the stimulation contact is that sensing of LFPs is separated from the stimulation electrode, which may result in one of the sensing electrodes being outside the STN.

This article has been accepted for publication in a future issue of this journal, but has not been fully edited. Content may change prior to final publication. Citation information: DOI 10.1109/TNSRE.2016.2613412, IEEE Transactions on Neural Systems and Rehabilitation Engineering

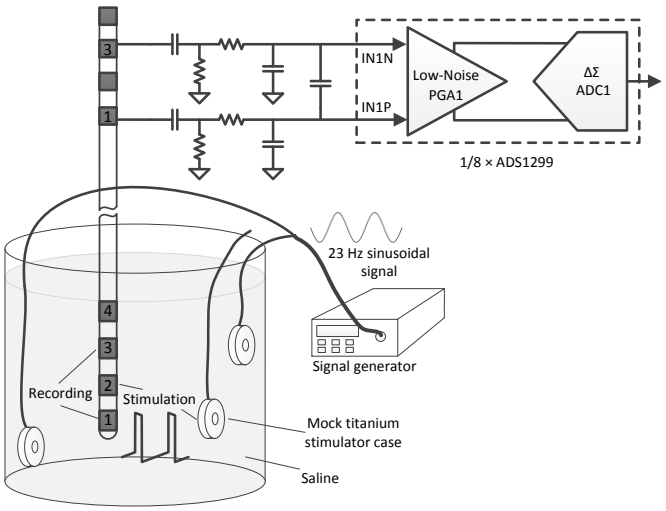

Fig. 1. Schematic of *in vitro* experimental setup used to record LFPs during DBS. A DBS lead was immersed in a saline bath for recording and to deliver stimulation. Two Ag/AgCl discoid electrodes were positioned on either side of the DBS lead to deliver the simulated LFP (23 Hz sinusoidal signal). Another Ag/AgCl discoid electrode positioned away from the DBS lead was used to mimic the metal case of the stimulator, which severed as the positive stimulation pole. Differential signal between electrode 1 and 3 was delivered to an analog front-end chip (ADS1299) after being passively band-pass filtered between 0.3 and 100 Hz.

C. Explanation of the signal chain

With the symmetric electrode configuration illustrated in Figure 1, the two recording electrodes sense approximately the same stimulation pulses. After passing through the filter network, the input signals were suppressed. The limited accuracies of the capacitor and resistor in the passive filter network, especially the capacitor, resulted as the mismatched elements transforming some of the common mode voltages into differential mode voltages. Mismatches between the electrode/tissue impedance also contribute to this. Thus, there are still several millivolt differential voltages remaining. This input differential signal was first amplified with a gain of 24 times and then modulated by the modulator of the delta-sigma ADC at a rate of 1.024 MHz. The digital decimation filter received the modulator output and decimated the data stream, which consisted of a third-order Sinc filter with the Z-domain transfer function

$$|H(z)| = |(1 - z^{-N})/(1 - z^{-1})|^3, \qquad (1)$$

where N is the decimation ratio.

D. Artifact removal

1) DBS artifact characterization

In most instances, the DBS artifact can be regarded as linear stationary signal. Based on the theory of Discrete Fourier Transforms, the spectrum content consists of harmonic frequency components that are integer multiples of the fundamental frequency. In addition to the harmonics, possible ADC aliasing brings in aliased artifact frequencies that can be determined from the sampling frequency. Thus, the harmonics and aliased artifacts can be easily identified for given stimulation and sampling frequencies. A signal recorded during the 2 V, 90 μs, 130 Hz stimulation in the saline solution was shown in figure 2A, and the signal recorded when the stimulation was OFF was also shown, which served as a reference, i.e., as a clean signal. The time domain waveform shows that a residual stimulation artifact at a high amplitude, more than two orders of magnitude greater than the desired signal. Figure 2B shows the power spectrum of the signal recorded during stimulation and that of the signal when the stimulation was OFF. Since a 23 Hz sinusoidal signal was injected into the saline solution to simulate the LFP, this frequency was a peak at 23 Hz in the power spectrum. It is expected that we get a power spectrum similar to that of the signal when the stimulator is OFF. However, the high energy of the stimulation artifact created the strong peaks at the stimulator frequency and its harmonics which disrupted the original baseline, so spectra with and without DBS in the beta band could not be compared directly. Therefore, in this section, we proposed a method to suppress the residual DBS artifacts during the following off-line data processing.

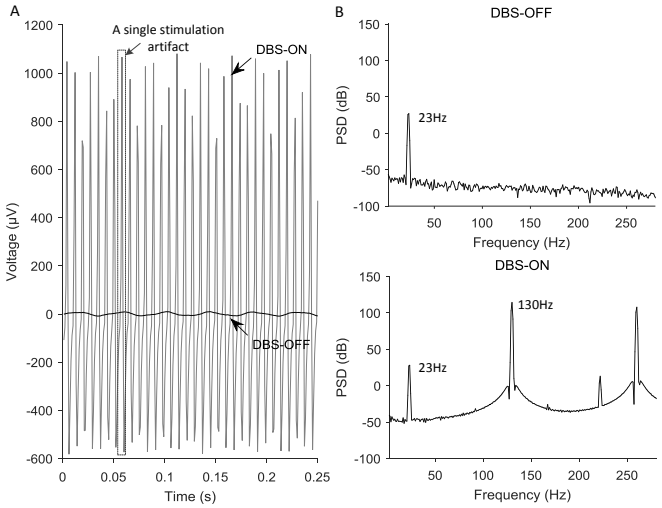

Fig. 2. Characteristics of stimulation artifacts. (A) Segments of 0.25 s of the original time signals recorded from the saline bath respectively when the DBS was OFF (black line) and when the DBS (2V, 130Hz, 90μs) was ON (grey line). The dashed line box indicates a single stimulation artifact. (B) The power spectrum of the signal when the DBS was OFF and the power spectrum of the signal when the DBS was ON. Note that the DBS artifact creates two strong peaks at the stimulation frequency and its harmonic.

2) Artifact removal methodology

As shown in figure 2A, the low sampling rate (1000Hz) resulted in each single stimulation artifact containing only a few data points (1000/stimulation frequency). Since the ratio of the sampling rate to the stimulation frequency might be not an integer, the morphology of the recorded stimulation artifacts varied. In addition, there were variations in the sampling rate and the stimulation frequency when accurately measured, possibly due to the limited accuracy of the system clock which further increased the variation of the stimulation artifacts in the time domain. For example, even though the DBS frequency was programmed to 130 Hz, the actual applied frequency would have a small deviation with the setting value. The variability of the stimulation artifact morphology made it difficult to directly extract a template from each single stimulation artifact waveform. Template subtraction using overlaying and averaging [22] is only applicable to signals recorded at high sampling rates where the stimulus artifact shape is invariable due to having an adequate number of

This article has been accepted for publication in a future issue of this journal, but has not been fully edited. Content may change prior to final publication. Citation information: DOI 10.1109/TNSRE.2016.2613412, IEEE Transactions on Neural Systems and Rehabilitation Engineering

sampling points. Hence, with a reverse thinking, a template rebuilding method was developed to remove the deep brain stimulation artifacts in the low sampling rate signal.

As explained in Part C, the delta-sigma ADC modulated the amplified differential signal at a high rate (1.024MHz) and then down-sampled it to 1 kHz after anti-aliasing filtering. Before down-sampling, the stimulation artifacts of the filtered signal were almost the same, so the basic strategy was to rebuild a single stimulation artifact of this stage by using the detrended raw recorded signal to extract the stimulation artifact template by the segmentation and overlaying of each artifact.

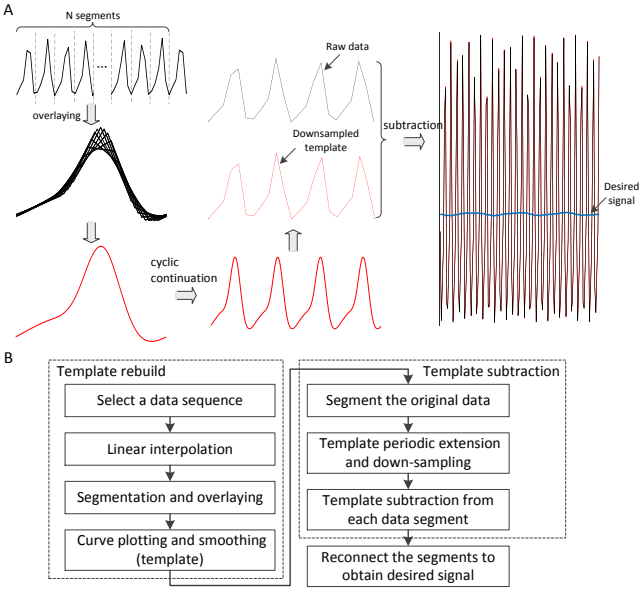

Fig. 3. A. Artifact removal by template subtraction from the original signal recorded from the saline bath during 180 Hz stimulation. A data sequence containing M data points from the detrended raw data was used for rebuilding the artifact template. This data sequence should approximately contain an integral number (denoted by N) of stimulation pulse artifacts, which was determined through comparing the shapes of the first stimulation pulse artifact and the one following this data sequence. A linear interpolation method was then used to increase the number of data points to the least common multiple of N and M (or N times M). This data sequence was then segmented into N segments with these segments overlapping. The raw data points in these N segments (not interpolation points) were then plotted out and smoothed to rebuild the single artifact waveform before the decimation procedure inside the Δ-Σ ADC. The rebuilt template was extended by cyclic continuation and then downsampled with a proper phase which defined a number of samples by which to offset. Finally the downsampled template was subtracted from the raw data to get the desired useful signal. Note that the schematic diagram here was simplified for demonstration. B. The general stimulation artifact removal procedure.

3) Artifact removal procedure

Figure 3B illustrates the stimulation artifact removal procedure.

A data sequence from the detrended raw data was used for building the artifact template. The EMD technique was used for detrending as described in [21]. This selected data sequence should contain approximately an integral number of stimulation pulse artifacts. The selection steps are as follows; first the peak point of each artifact in the detrended raw data was found out and marked by peak detection. Then designate an artifact (or its peak point) as one end, and next it is expected to find a very similar artifact as it, thus we generally think that there are approximately an integral number of stimulation pulse artifacts between them. To find out this very similar artifact, we first exclude a few peak points by excluding the points with a value divergence between them and the chosen peak point exceeding a set threshold value. The chosen artifact shape was then compared to shapes of the remaining artifacts one by one to find the very similar one by searching the one with minimum average deviation of artifact point value. That is to find the artifact satisfying

$$min \sum |d_n - d_n'| , \quad (2)$$

where *min* stands for find the minimum value, and d_n and d_n' are the data points of the two compared artifacts, and n is the index of the data point of each artifact. Thus we got a data sequence which contained approximately an integral number of stimulation pulse artifacts.

The number of stimulation pulse artifacts in this data sequence is denoted by N and the number of data points is denoted by M. For the next segmentation process, a linear interpolation method was then used to increase the number of data points to the least common multiple of N and M (or N times M). This data sequence was then divided into N segments, with these segments overlapping. The raw data points in the N segments (not interpolation points) were plotted out. The plotted line was then smoothed using a moving average filter to rebuild the artifact template.

After the template building, the artifact template was to be subtracted from the raw data. The steps were as follows; the template was subtracted in segments with the raw data divided into several segments. The subtraction method first extended the rebuilt template by cyclic continuation, according to the raw data segment length. The extended template was then downsampled, which was keeping every *m*th sample starting with the first point with a specific phase. The *m* equals the number of data points of a single artifact template divided by the M. And finally the downsampled template was subtracted from the raw data. Here it was important that the downsampling of the extended template needed to specify the phase, which is the number of samples by which to offset, as the downsampled template should be aligned to raw data segment. This was achieved by aligning the first artifacts, respectively, of the extended template and the raw data segment. The first point to be decimated was one of the points of the first artifact of the extended temple. We attempted to make the first downsampled artifact have a minimum deviation with the first artifact of the raw data segment to decide the first point to be decimated. Therefore, the screening criteria (2) was also be used for finding the offset of downsampling. There should be a large computation if compared point by point, so the offset (or the first point to be decimated) was found by gradually narrowing the range to minimize the total difference between each data point of the two first stimulation artifacts, respectively, of the downsampled template and the raw data. The last step reconnected the segments after subtraction to obtain the desired signal.

E. In vivo experiment

1) Patients and Surgical procedures

The artifact removal method was also tested in a clinical trial.

The clinical data was recorded from 26 participants with bilateral or unilateral STN-DBS after lead implantation during an operation after a 12-hour withdrawal from all Parkinsonian medications or in the ward during a DBS therapy test. All subjects demonstrated typical Parkinsonian motor symptoms, including akinesia, rigidity, and tremors. All subjects gave their written informed consent before participating in the study and all the procedures were approved by the ethics committee of the Beijing Tiantan Hospital, Capital Medical University. Implantation was performed under local anesthesia. All subjects received the same model DBS lead (L301, Pins Medical, CHA) with stereotactic imaging, microelectrode recording, and macro-stimulation to place the electrodes into the STN.

2) Data Collection

STN LFPs were directly recorded from the DBS electrode contacts connected to a twist-lock cable (model A601-07, Pins Medical, CHA) at the completion of the DBS electrode insertion and testing. Previous studies used symmetric geometry to record differential LFPs on the same lead with unipolar stimulation as described in [17], where authors used a gel electrode pad that was placed over the left clavicle as DBS cathode and recorded across the neighbour electrodes closest to the anodic stimulation electrode in their adaptive DBS system. However, the impedance of the skin is a little large and not very stable if the gel pad is not stable. In this study, bipolar stimulation configuration was used instead of a unipolar mode, as stimulation pulses was applied between electrode 4+ and 2-. The differential signal was recorded between the contacts 1 and 3 at a sampling rate of 1000 Hz. The study aimed to study the relationship between the DBS parameters and the STN LFP variation. To minimize the total time during the operation, a pre-programed stimulation program was used to automatically change the stimulation parameters. Each recording period following the DBS electrode testing stage consisted of several seconds baseline DBS-OFF period, followed by several LFP segments during stimulation with different parameters. The recording time of each segment was 5 seconds to minimize the impact on the DBS surgery. 14 data sets were for the effect of the DBS frequency, 21sets were for the effect of the DBS amplitude, and 5 sets were for the effect of the DBS pulse width. The stimulation parameters listed in table 1 generally cover the parameters commonly used in clinical treatments.

TABLE I
THE STIMULATION PARAMETERS FOR STUDY OF THE RELATIONSHIP BETWEEN DBS PARAMETERS AND STN LFP

Parameters	VALUES
Stimulation Frequency	60 Hz, 70 Hz, 80 Hz, 90 Hz, 100 Hz, 110 Hz, 120 Hz, 130 Hz, 135 Hz, 140 Hz, 145 Hz, 150 Hz, 155 Hz, 160 Hz, 165 Hz, 170 Hz, 175 Hz, 180 Hz, and 185 Hz with pulse amplitudes of 1.5 V, 2 V, and 3 V with a fixed pulse width of 90 μs
Pulse Amplitude	1 V–3 V in increments of 0.1 V with a fixed pulse width and frequency
Pulse width	60 and 90 μs with a fixed pulse frequency for each listed amplitude above

F. Data analysis

1) Frequency spectrum analysis

All the analyses in this study were realized offline using MATLAB version R2014a (The Mathworks, Natick, MA, USA). The power spectra for the various frequencies were estimated using Welch's averaged modified periodogram method [24]. Each segment of the signal was divided into sections of 1000 samples with overlaps of 1000*0.5 samples and all sections were Hanning windowed. The frequency resolution was approximately 1 Hz. 4 second data sets were used for spectrum analyses.

2) Quantitative evaluation

The effect of the artifact removal method was evaluated using a quantitative measure in addition to visual inspection. After artifact removal the power spectrum of the recovered useful signal during DBS ON should be very similar to the power spectrum of the signal when the stimulation is OFF. This was evaluated through the ratio R, expressed in decibels (dB), computed as:

$$R = \mathrm{mean}_f\left(\left|10 \cdot \log_{10}\left(\frac{P_{OFF}(f)}{P_{ON}(f)}\right)\right|\right), \quad (3)$$

where $P_{OFF}(f)$ and $P_{ON}(f)$ denote the power spectrum of the signal when the stimulation is OFF and the recovered useful signal during DBS ON at each frequency f, and mean_f corresponds to the arithmetic mean over all frequencies. Some useful LFP biomarkers for DBS applications usually have frequencies below 100 Hz, such as the frequency range for PD which is the beta band. Thus R was computed in the frequency range of 3~100 Hz.

For the *in vivo* tests, statistics on the beta power ratio were calculated at the group level. To evaluate the dependence relationship of the STN beta power attenuation on the DBS parameters, linear regression was performed separately for the beta power ratio of recordings during DBS relative to its baseline for each case. The beta power ratio was computed according to the following equation:

$$\text{Raw beta power ratio} = 10 \cdot \log 10(\beta_{stim}/\beta_{baseline}), \quad (4)$$

3) Statistical analysis

Data were not normally distributed so that beta band suppressions were compared using the nonparametric Wilcoxon's signed rank tests. Results are reported as mean ± standard error of the mean (SEM). Pearson correlation coefficient was calculated to evaluate the relationship between the stimulation parameters and the beta band suppression degree.

III. RESULTS

A. In vitro experiment

1) Time domain analysis

The signal segments recorded from the saline water during DBS ON are compared with segments when the DBS was OFF in figure 4A and B. The original DBS-ON signal almost completely obscures the useful sinusoidal signal because of the large stimulation artifact. However, removed of the stimulation artifact gave the nearly sinusoidal signal shown in figure 4C, although some slight residual stimulation artifacts still remained in the visual inspection of the time domain signals.

This article has been accepted for publication in a future issue of this journal, but has not been fully edited. Content may change prior to final publication. Citation information: DOI 10.1109/TNSRE.2016.2613412, IEEE Transactions on Neural Systems and Rehabilitation Engineering

The next section explains the quantitative evaluation in the frequency domain.

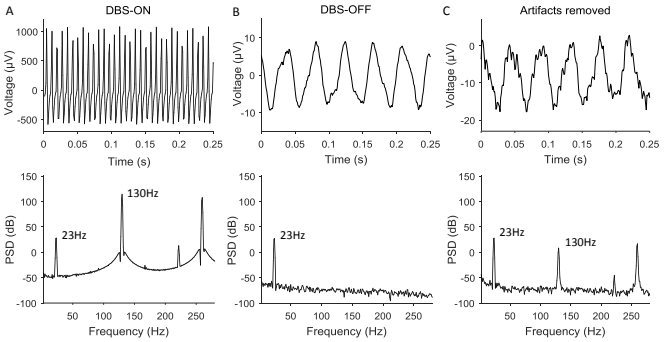

Fig. 4. Segments of 0.25 s of the original time signals recorded from the saline bath and the power spectra of them. (A) Signal when DBS (2V, 130Hz, 90μs) is ON. (B) Signal when DBS is OFF. (C) Signal after artifacts removal.

2) Frequency domain analysis

Figure 4A and C shows the power spectrum of the raw signal and the signal after artifact removal. The proposed artifact removal suppresses the DBS artifact with the baseline brought to the original level with only some residual stimulation artifacts. The peaks at 23 Hz, the injected sinusoid frequency is still evident. A notch filter has been used for removing the power line interference. The ratio R between the signal recorded when the stimulation was OFF and the raw signal recorded when the stimulation ON is 3.30, while the ratio between the signal without stimulation and the signal after artifact removal is 0.47. A Butterworth ten-order low-pass filter with a cutoff frequency of 100 Hz was also applied to the original signal, giving a ratio of 0.73. Obviously, the closer to zero the ratio is, the better the artifacts are suppressed.

3) Effect of stimulation parameters and sampling frequency

The stimulation artifact removal was also tested with different DBS parameters and sampling frequencies with the results shown in figure 5. Each parameter was chosen according to typical clinical values, although the choices were not exhaustive. The parameter combination of 150 Hz stimulation frequency, 90 μs pulse width, 2 V pulse amplitude and 1000 Hz sampling frequency was used as the base case with the parameters then varied one at a time. As shown in figure 5, increasing the stimulation frequency slightly reduced the ratio R, while increasing the pulse width, increasing the pulse amplitude and increasing the sampling rate all increased R. The artifact removal method improved the signals in all cases with the ratio R induced to near zero in all cases, indicating that the artifacts were well suppressed.

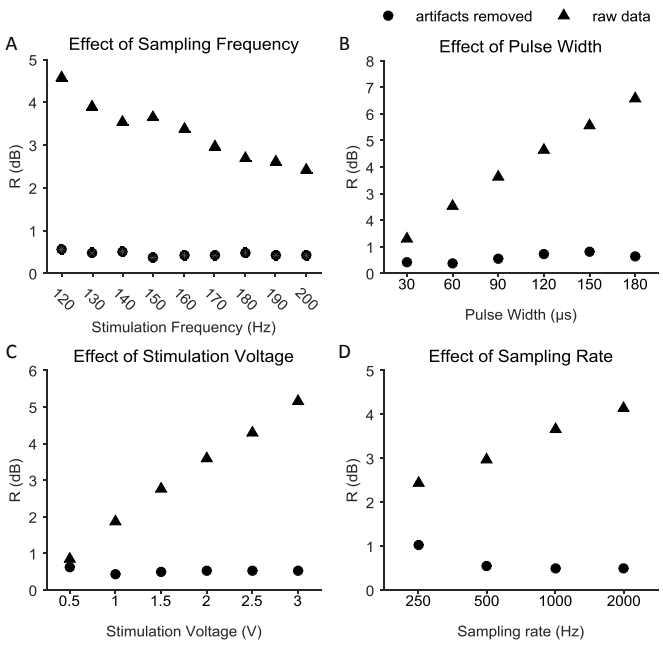

Fig. 5. Effect of varying simulation parameters and sampling rates on the performance of artifacts removal approach. (A) Stimulation frequency. (B) Pulse width. (C) Stimulation voltage. (D) Sampling rate. The parameter combination of 150 Hz stimulation frequency, 90 μs pulse width, 2 V pulse voltage and 1000 Hz sampling rate was used as the base case with the parameters then varied one at a time. Each triangular plot stands for the original ratio R for each parameter combination, and each circular plot stands for the ratio R after artifacts removal. Note that increasing the stimulation frequency slightly induced the ratio R, while increasing the pulse width, increasing the pulse amplitude and increasing the sampling rate all increased ratio R. The artifact removal method improved the signals in all cases with the ratio R induced to near zero in all cases, indicating that the artifacts were well suppressed.

B. In vivo experiment

The STN LFPs of the PD patients were recorded by the proposed recording system, and the LPFs with DBS ON were processed to remove artifacts. The tests examined how the LFP characteristics were dependent on the stimulation parameters.

1) Pulse Amplitude

The DBS mode was programed to use various amplitudes for a constant stimulation frequency with the stimulation amplitude increased gradually from 1.0 V to 3.0 V with a step of 0.1 V. The time-evolving short-time Fourier transform taken at 0.2 s intervals of the STN LPF from one side of a Parkinson's disease patient shown in figure 6A and the time-evolving beta band power shown in figure 6B show suppression of the beta band LFP peaks with increasing DBS pulse voltage. The signal when DBS was OFF is presented to show the excessive power in the beta band. The time-evolving spectrograms show suppression of the beta band LFP peaks with increasing DBS voltage, with the beta band oscillations gradually retrieving when stimulation was off. Figure 7 shows the attenuation of the beta band power ratio as a function of the DBS voltage within the STN. The results showed that in the stimulation voltage range of 1 V to 3 V, the degree of β band power inhibition increased with increasing stimulation voltage during DBS-ON within the STN.

This article has been accepted for publication in a future issue of this journal, but has not been fully edited. Content may change prior to final publication. Citation information: DOI 10.1109/TNSRE.2016.2613412, IEEE Transactions on Neural Systems and Rehabilitation Engineering

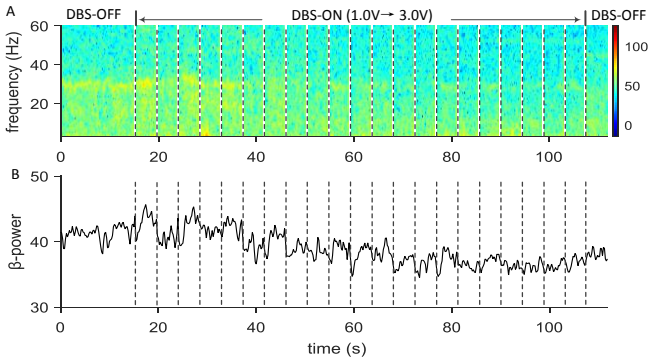

Fig. 6. An example of the clinical data recorded from the STN of a PD patient. This data contains a period of stimulation with gradually increasing voltages. (A) Time-evolving spectrogram of the STN-LFP using short-time Fourier transform. (B) Time-evolving β band power of each segment of the LFP during DBS for various stimulation voltages with a time resolution of 0.2s.

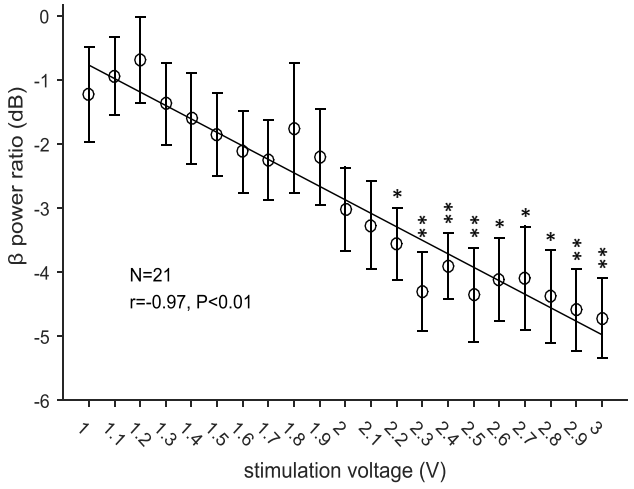

Fig. 7. β band power suppression induced by various stimulation voltage with fixed stimulation frequency and pulse width. A ratio was taken between β power when DBS was ON and that when DBS was OFF. Each circular plot stands for the group average value of log β band power ratios of 21 datasets at each stimulation voltage and each bar stands for the SEM. Significant difference was tested between the suppression of 1V with the those of other voltages; *P<0.05, **P<0.01 (Wilcoxon signed rank test). Note that the degree of β band power inhibition increased in a voltage-dependent fashion during stimulation within the STN. The correlation coefficient between the ratio average values and the stimulation voltages is -0.97 (Pearson's rank; P<0.01).

2) Stimulation Frequency

The effect of the DBS frequency on the pathological synchrony in the subthalamic region was studied by recording the STN LFPs during stimulation with sweep frequencies from 60 Hz to 185 Hz at amplitudes of 1.5 V, 2 V, and 3 V. Comparison of the power spectra between the DBS-OFF and DBS-ON states showed that the group beta power was attenuated in a frequency-dependent tendency during the DBS. Figure 8 shows the beta power attenuation as a function of the frequency for the 1.5 V DBS, 2 V DBS and 3 V DBS in the STN. The beta power decreases with increasing frequency within a frequency range of 60 to 120 Hz. When the stimulation frequency was programmed to the clinically commonly used high frequency range which is about 120 to 185Hz, beta power didn't present an obvious declining trend anymore, indicating a mechanism of effectiveness of high frequency stimulation (HFS).

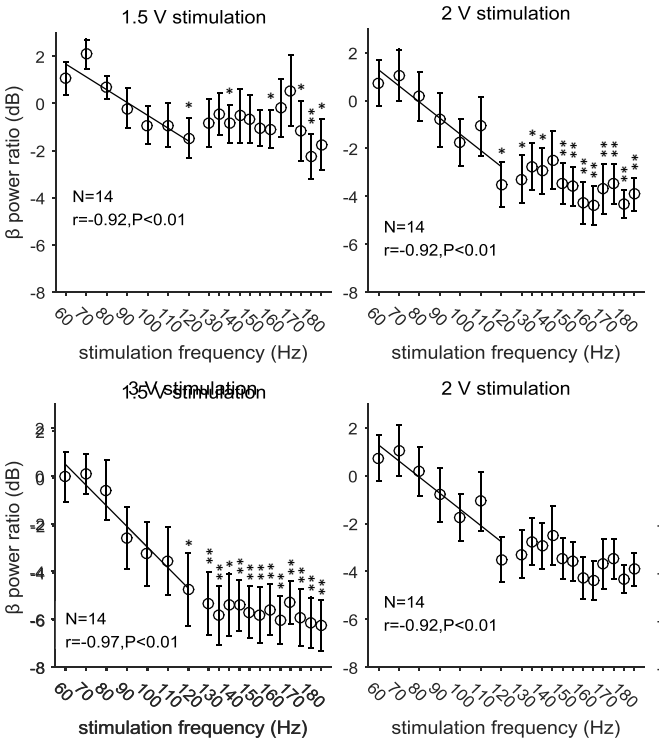

Fig. 8. β band power suppression induced by various stimulation frequency respectively with1.5V, 2V and 3V voltage, with a fixed stimulation pulse width. Each circular plot stands for the group average value of log β band power ratios of 14 datasets at each parameter combination and each bar stands for the SEM. Significant difference was tested between the suppression of 60Hz with the those of other frequencies; *P<0.05, **P<0.01 (Wilcoxon signed rank test). Note that the degree of β band power inhibition increased with increasing frequency within the range of 60 to 120Hz. The correlation coefficient between the ratio average values and the stimulation frequency in this range was analyzed respectively.

3) Pulse width

The effect of pulse widths was tested for each sweeping stimulation voltage for 60 μs and 90 μs pulse widths, which were most commonly used in clinical practice. Figure 9 shows the valuation of the suppression for the two pulse widths for various stimulation voltages, which shows that the beta power ratio of the wider pulse width was smaller. However, no statistically significant difference was found between the beta band suppression of 60 μs and 90 μs pulse widths in each group with fixed stimulation voltage.

This article has been accepted for publication in a future issue of this journal, but has not been fully edited. Content may change prior to final publication. Citation information: DOI 10.1109/TNSRE.2016.2613412, IEEE Transactions on Neural Systems and Rehabilitation Engineering

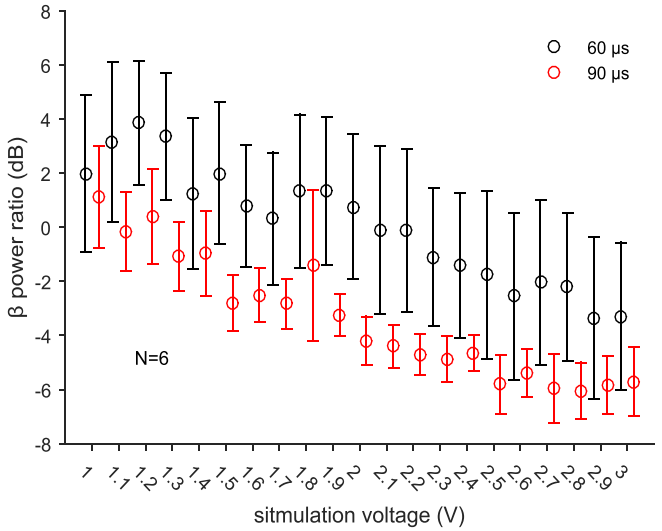

Fig. 9. β band power suppression induced by 60μs and 90μs with each stimulation voltage. Each circular plot stands for the group average value of log β band power ratios of 6 datasets (red for 60μs, and black for 90μs) and the bars stand for SEMs. 90μs stimulation showed more suppression of β band power than 60μs stimulation, but no significant difference was found between them with each stimulation voltage.

IV. Discussion

Previous DBS device are unable to accurately record the LFP during stimulation due to the high pulse amplitude, high frequency, stringent duty cycles in typical DBS therapies. However, Rossi et al. [9] developed a system called 'FilterDBS' which could record artifact-free LFPs during DBS which minimized the time delay in measuring the biomarker response to stimulations. This technique has been used to confirm similar effects as with dopamine that DBS electrode stimulation suppressed excessive beta synchronization in the subthalamic nucleus (STN) in PD patients [10, 11], which has been widely accepted as a potential biomarker of PD [12]. As a research tool, the 'FilterDBS' system had a limited bandwidth of just 2~40 Hz restrained studies on the wider frequency range of electrophysiological activities such as the gamma band (30~70 Hz) activity, whereas studies have found that when patients with PD are treated with dopaminergic medication, the beta band power of the LFPs is greatly decreased, but is replaced by increased oscillations in the high-gamma band [13, 14].

As there is an increase in the aging populations and the number of brain disorders, the monitoring of long-term brain electrophysiological activities, especially for patients with psychiatric diseases and AD, is important because researchers know little about these diseases [30]. This study describes a signal processing method for the stimulation artifacts removal, which was designed for the off-line data processing based on a platform of implantable recording of LFP during simultaneous DBS in our previous study [20], providing insights into the synchronized neural activity directly affected by the stimulation. The proposed method for stimulation artifacts removal was validated using a salt solution model and intraoperatively *in vivo* tested in PD patients.

The present study is restricted due to several limitations. Firstly, although the artifact removal method drastically suppressed the stimulation artifacts, there were still some small remaining artifacts. This may be a result of two possible causes. The first cause may be the slight fluctuations of the stimulation waveforms over time. There will be some slight deviations between the pulse waveforms due to the analog circuit characteristics; therefore, the recorded stimulation artifacts are not constant and each artifact does not exactly match the template. The second possible reason may be the inaccuracy of the reconstructed template. The artifact template was reconstructed using the raw recorded signal, which also contained the desired useful signal. Also, the method tries to select a signal segment containing an integer number of artifacts, but may not accurately capture an integer number of cycles. As a consequence, the rebuilt template may be slightly inaccurate which would lead to residual artifacts after the template extraction. In addition, the artifact removal method proposed in this article at present can only be used for the offline data processing. Further studies on the real-time hardware implementation should be done for the application of the closed-loop DBS. The second limitation is that the tests to study how the LFP characteristics depend on the stimulation parameters were limited by the total testing time during the DBS operation, so there was no DBS-OFF segment to "restore" the brain activity between adjacent segments with different DBS sweep frequencies and amplitudes. Some studies have suggested that electrical modulation of neural activity brought about temporal effect [26, 27], which after the DBS is turned off it takes some time before the beta band pathological oscillations to return and the elution time is related with the stimulation duration. Therefore, to avoid the previous stimulation caused effect being added to the next stimulation periods with different parameter settings, there should be more than several seconds in time between the adjacent stimulation to enable the pathophysiological synchronization to come back. However, this was omitted in this study due to a limited testing time and large amount of stimulation parameters tested, which may somewhat influence the results. Also, each segment was not very long, so long-term effects may not have been reflected. In addition, due to intraoperative restriction this study lacked a behavioral assessment that might have allowed association of the stimulation parameters inducing the suppressed beta band oscillations and the objectively improved motor performance in all patients. In fact, previous studies have demonstrated that 95% PD patients show significant beta band oscillation in the LFP of their basal ganglia and when they receive dopaminergic pharmacotherapy, this oscillation will be suppressed and the improvement of bradykinesia and rigidity by pharmacotherapy is related with the degree of suppression [29]. Future studies can compare the movement improvements as seen in pharmacological treatments with the quantitative dependences of beta band synchronization variations in the STN on the DBS parameters.

V. Conclusions

The present study proposed a novel approach for removing stimulation signal artifacts, providing off-line data processing for devices with the function of sensing neural electrical activity such as LFPs while providing deep brain stimulation

therapy. The results of in vitro experiments indicate that the stimulation artifacts are well suppressed after template subtraction. On this basis, we explored the quantitative dependences of beta band synchronization variations in the STN on the applied DBS parameters in PD patients. DBS therapy suppresses excessive beta band frequency activity with the attenuation increasing with increasing DBS voltage and increasing DBS frequency within a range of 60 to 120 Hz. Beta power didn't present an obvious declining trend anymore in the frequency range of about 120 to 185Hz. 90μs stimulation showed more suppression of β band power than 60μs stimulation, but no significant difference was found between them. This study may maximize the efficacy by associating the synchronized neural activity variability directly affected by the stimulation with the therapy dose. The proposed artifact suppression method provides technical support for exploring the instantaneous effect of electrical stimulation on the brain activities.

REFERENCES

[1] M. L. Kringelbach, N. Jenkinson, S. L. Owen, and T. Z. Aziz, "Translational principles of deep brain stimulation," *Nature Reviews Neuroscience*, vol. 8, no. 8, pp. 623-635, 2007.

[2] S. Miocinovic, S. Somayajula, S. Chitnis, and J. L. Vitek, "History, applications, and mechanisms of deep brain stimulation," *JAMA neurology*, vol. 70, no. 2, pp. 163-171, 2013.

[3] A. Abosch, D. Lanctin, I. Onaran, L. Eberly, M. Spaniol, and N. F. Ince, "Long-term recordings of local field potentials from implanted deep brain stimulation electrodes," *Neurosurgery*, vol. 71, no. 4, pp. 804-814, 2012.

[4] G. Giannicola, M. Rosa, D. Servello, C. Menghetti, G. Carrabba, C. Pacchetti, R. Zangaglia, F. Cogiamanian, E. Scelzo, and S. Marceglia, "Subthalamic local field potentials after seven-year deep brain stimulation in Parkinson's disease," *Experimental neurology*, vol. 237, no. 2, pp. 312-317, 2012.

[5] J. A. Thompson, D. Lanctin, N. F. Ince, and A. Abosch, "Clinical Implications of Local Field Potentials for Understanding and Treating Movement Disorders," *Stereotactic and functional neurosurgery*, vol. 92, no. 4, pp. 251-263, 2014.

[6] M. Alegre, and M. Valencia, "Oscillatory activity in the human basal ganglia: More than just beta, more than just Parkinson's disease," *Experimental neurology*, vol. 248, pp. 183-186, 2013.

[7] H. Tan, A. Pogosyan, A. Anzak, T. Foltynie, P. Limousin, L. Zrinzo, K. Ashkan, M. Bogdanovic, A. L. Green, and T. Aziz, "Frequency specific activity in subthalamic nucleus correlates with hand bradykinesia in Parkinson's disease," *Experimental neurology*, vol. 240, pp. 122-129, 2013.

[8] M. S. Okun, "Deep-Brain Stimulation—Entering the Era of Human Neural-Network Modulation," *New England Journal of Medicine*, vol. 371, no. 15, pp. 1369-1373, 2014.

[9] L. Rossi, G. Foffani, S. Marceglia, F. Bracchi, S. Barbieri, and A. Priori, "An electronic device for artefact suppression in human local field potential recordings during deep brain stimulation," *Journal of neural engineering*, vol. 4, no. 2, pp. 96, 2007.

[10] L. Rossi, S. Marceglia, G. Foffani, F. Cogiamanian, F. Tamma, P. Rampini, S. Barbieri, F. Bracchi, and A. Priori, "Subthalamic local field potential oscillations during ongoing deep brain stimulation in Parkinson's disease," *Brain research bulletin*, vol. 76, no. 5, pp. 512-521, 2008.

[11] A. Eusebio, W. Thevathasan, L. D. Gaynor, A. Pogosyan, E. Bye, T. Foltynie, L. Zrinzo, K. Ashkan, T. Aziz, and P. Brown, "Deep brain stimulation can suppress pathological synchronisation in parkinsonian patients," *Journal of Neurology, Neurosurgery & Psychiatry*, vol. 82, no. 5, pp. 569-573, 2011.

[12] R. Levy, P. Ashby, W. D. Hutchison, A. E. Lang, A. M. Lozano, and J. O. Dostrovsky, "Dependence of subthalamic nucleus oscillations on movement and dopamine in Parkinson's disease," *Brain*, vol. 125, no. 6, pp. 1196-1209, 2002.

[13] P. Silberstein, A. A. Kühn, A. Kupsch, T. Trottenberg, J. K. Krauss, J. C. Wöhrle, P. Mazzone, A. Insola, V. Di Lazzaro, and A. Oliviero, "Patterning of globus pallidus local field potentials differs between Parkinson's disease and dystonia," *Brain*, vol. 126, no. 12, pp. 2597-2608, 2003.

[14] P. Brown, and D. Williams, "Basal ganglia local field potential activity: character and functional significance in the human," *Clinical neurophysiology*, vol. 116, no. 11, pp. 2510-2519, 2005.

[15] B. Rosin, M. Slovik, R. Mitelman, M. Rivlin-Etzion, S. N. Haber, Z. Israel, E. Vaadia, and H. Bergman, "Closed-loop deep brain stimulation is superior in ameliorating parkinsonism," *Neuron*, vol. 72, no. 2, pp. 370-384, 2011.

[16] S. Santaniello, G. Fiengo, L. Glielmo, and W. M. Grill, "Closed-loop control of deep brain stimulation: a simulation study," *Neural Systems and Rehabilitation Engineering, IEEE Transactions on*, vol. 19, no. 1, pp. 15-24, 2011.

[17] S. Little, A. Pogosyan, S. Neal, B. Zavala, L. Zrinzo, M. Hariz, T. Foltynie, P. Limousin, K. Ashkan, and J. FitzGerald, "Adaptive deep brain stimulation in advanced Parkinson disease," *Annals of neurology*, vol. 74, no. 3, pp. 449-457, 2013.

[18] S. Stanslaski, P. Afshar, P. Cong, J. Giftakis, P. Stypulkowski, D. Carlson, D. Linde, D. Ullestad, A.-T. Avestruz, and T. Denison, "Design and validation of a fully implantable, chronic, closed-loop neuromodulation device with concurrent sensing and stimulation," *Neural Systems and Rehabilitation Engineering, IEEE Transactions on*, vol. 20, no. 4, pp. 410-421, 2012.

[19] H. Shen, "Neuroscience: Tuning the brain," *Nature News & Comment*, vol. 507, no. 7492, pp. 290-292, 2014

[20] X. Qian, H. Hao, B. Ma, X. Wen, C. Hu, and L. Li, "Implanted rechargeable electroencephalography (EEG) device," *Electronics Letters*, vol. 50, no. 20, pp. 1419-1421, 2014.

[21] A. Santillan-Guzman, U. Heute, M. Muthuraman, U. Stephani, and A. Galka, "DBS artifact suppression using a time-frequency domain filter." pp. 4815-4818.

[22] T. Hashimoto, C. M. Elder, and J. L. Vitek, "A template subtraction method for stimulus artifact removal in high-frequency deep brain stimulation," *Journal of neuroscience methods*, vol. 113, no. 2, pp. 181-186, 2002.

[23] "Low-Noise, 8-Channel, 24-Bit Analog Front-End for Biopotential Measurements," Texas Instruments 2012.

[24] P. D. Welch, "The use of fast Fourier transform for the estimation of power spectra: A method based on time averaging over short, modified periodograms," *IEEE Transactions on audio and electroacoustics*, vol. 15, no. 2, pp. 70-73, 1967.

[25] A. Fasano, and A. M. Lozano, "The FM/AM world is shaping the future of deep brain stimulation," *Movement Disorders*, vol. 29, no. 2, pp. 161-163, 2014.

[26] B. Wingeier, T. Tcheng, M. M. Koop, B. C. Hill, G. Heit, and H. M. Bronte-Stewart, "Intra-operative STN DBS attenuates the prominent beta rhythm in the STN in Parkinson's disease," *Experimental neurology*, vol. 197, no. 1, pp. 244-251, 2006.

[27] H. Bronte-Stewart, C. Barberini, M. M. Koop, B. C. Hill, J. M. Henderson, and B. Wingeier, "The STN beta-band profile in Parkinson's disease is stationary and shows prolonged attenuation after deep brain stimulation," *Experimental neurology*, vol. 215, no. 1, pp. 20-28, 2009.

[28] A. R. Kent, W. M. Grill W M, "Recording evoked potentials during deep brain stimulation: development and validation of instrumentation to suppress the stimulus artefact," *Journal of neural engineering*, vol. 9, no. 3, pp. 036004, 2012.

[29] N. J. Ray, N. Jenkinson, S. Wang, P. Holland, J. S. Brittain, C. Joint, J. F. Stein and T.Aziz, "Local field potential beta activity in the subthalamic nucleus of patients with Parkinson's disease is associated with improvements in bradykinesia after dopamine and deep brain stimulation," *Experimental neurology*, vol. 213 , no. 1, pp. 108-113, 2008.

[30] H. Shen, "Tuning the brain," *Nature* , vol. 507, pp. 290-292, 2014.